



Research Article

A Mouse Model That Reproduces the Developmental Pathways and Site Specificity of the Cancers Associated With the Human *BRCA1* Mutation Carrier State



Ying Liu^a, Hai-Yun Yen^b, Theresa Austria^a, Jonas Pettersson^a, Janos Peti-Peterdi^c, Robert Maxson^b, Martin Widschwendter^d, Louis Dubeau^{a,*}

^a Department of Pathology, Keck School of Medicine of University of Southern California, Los Angeles, CA 90089, United States

^b Department of Biochemistry and Molecular Biology, Keck School of Medicine of University of Southern California, Los Angeles, CA 90089, United States

^c Department of Physiology and Biophysics, Keck School of Medicine of University of Southern California, Los Angeles, CA 90089, United States

^d Department of Women's Cancer, University College London, London, UK

ARTICLE INFO

Article history:

Received 24 July 2015

Received in revised form 22 August 2015

Accepted 26 August 2015

Available online 9 September 2015

Keywords:

Brc1

Familial cancer predisposition

Müllerian inhibiting substance

Mouse model of breast and ovarian cancer

Cell non-autonomous mechanism of cancer predisposition

ABSTRACT

Predisposition to breast and extrauterine Müllerian carcinomas in *BRCA1* mutation carriers is due to a combination of cell-autonomous consequences of *BRCA1* inactivation on cell cycle homeostasis superimposed on cell-nonautonomous hormonal factors magnified by the effects of *BRCA1* mutations on hormonal changes associated with the menstrual cycle. We used the Müllerian inhibiting substance type 2 receptor (*Mis2r*) promoter and a truncated form of the Follicle stimulating hormone receptor (*Fshr*) promoter to introduce conditional knockouts of *Brc1* and *p53* not only in mouse mammary and Müllerian epithelia, but also in organs that control the estrous cycle. Sixty percent of the double mutant mice developed invasive Müllerian and mammary carcinomas. Mice carrying heterozygous mutations in *Brc1* and *p53* also developed invasive tumors, albeit at a lesser (30%) rate, in which the wild type alleles were no longer present due to loss of heterozygosity. While mice carrying heterozygous mutations in both genes developed mammary tumors, none of the mice carrying only a heterozygous *p53* mutation developed such tumors ($P < 0.0001$), attesting to a role for *Brc1* mutations in tumor development. This mouse model is attractive to investigate cell-nonautonomous mechanisms associated with cancer predisposition in *BRCA1* mutation carriers and to investigate the merit of chemo-preventive drugs targeting such mechanisms.

© 2015 The Authors. Published by Elsevier B.V. This is an open access article under the CC BY-NC-ND license (<http://creativecommons.org/licenses/by-nc-nd/4.0/>).

1. Introduction

Extra-uterine high-grade serous Müllerian carcinomas, which include cancers originating in either the fallopian tubes or endosalpingiosis (Dubeau, 2008; Dubeau and Drapkin, 2013), are the most lethal gynecological cancers while carcinomas of the breast are the most common cancer in women (Boyle et al., 2008). There is considerable overlap in the risk factors associated with both diseases. For example, menstrual cycle activity is the most important risk factor for the sporadic forms of both diseases while germline *BRCA1* or *BRCA2* mutations are the most important cause of the familial forms (Whittemore et al., 1992; Brose et al., 2002; Pike et al., 2004). An understanding of the underlying mechanisms mediating cancer risk for both diseases could have a significant impact on their morbidity and mortality by leading to the development of preventive strategies targeting these mechanisms specifically.

Existing mouse models for serous extra-uterine Müllerian (previously referred to as serous ovarian) carcinomas (Dubeau, 2008;

Dubeau and Drapkin, 2013), are based on forced expression of selected oncogenes, often combined with homozygous knockouts of *BRCA1* or *BRCA2* or other relevant tumor suppressor genes in a tissue-specific manner (Miyoshi et al., 2002; Orsulic et al., 2002; Connolly et al., 2003; Flesken-Nikitin et al., 2003; Dinulescu et al., 2005; Clark-Knowles et al., 2007; Szabova et al., 2012; Perets et al., 2013). None of these models, to our knowledge, are associated with predisposition to both reproductive and mammary cancers. These models have led to significant progress in establishing the role of the targeted genes or pathways in cancer development and elucidating their intracellular activity, but were not designed to investigate the interplay between environmental/hormonal and genetic factors. In addition, although heterozygous germline *BRCA1/2* mutations are strongly associated with cancer predisposition in both organs in human, the current models are invariably based on homozygous inactivation of these genes, a condition that is never present in the human germline. Even when restricted to specific organs, such homozygous lesions may lead to development defects in these organs (Xu et al., 1999; Kim et al., 2006), diminishing their relevance to human. The higher penetrance of homozygous mutations may also override the influence of environmental or

* Corresponding author at: Ezzalaw Tower #6338, 1441 Eastlake Avenue, Los Angeles, CA 90089, United States.

E-mail address: ldubeau@usc.edu (L. Dubeau).

systemic hormonal factors, thus complicating studies of their interaction with genetic factors. Finally, there is strong evidence, both from animal and human studies (Chodankar et al., 2005; Hong et al., 2010; Widschwendter et al., 2013), that *BRCA1* mutations lead to cancer predisposition not only via cell-autonomous mechanisms, but also via alterations in hormone producing cells that influence, from a distance, the cells from which ovarian and breast cancers develop. This conclusion is strengthened by the fact that menstrual cycle activity has a strong influence on risk of breast and extra-uterine Müllerian carcinoma, even in individuals with strong genetic predisposition such as *Brcal* mutation carriers (Narod et al., 1998). Current animal models based on inactivation of *Brcal* to induce the development of invasive cancers do not recapitulate such cell-nonautonomous mechanisms.

We sought to develop a mouse model for breast and extra-uterine Müllerian cancer predisposition based on conditional inactivation of *Brcal* not only in these organs, but also in hormone producing cells that regulate the menstrual cycle, including ovarian granulosa cells and the anterior pituitary gland, in order to mimic both the genetic background and the cell-nonautonomous conditions associated with strong predisposition to these cancers in humans. Transgenic constructs driving expression of Cre recombinase under the control of a combination of cell-specific promoters active in the various tissues of interest were introduced in mice carrying floxed alleles not only in *Brcal*, but also in *p53*, a gene mutated in almost all human cancers associated with the *BRCA1* mutation carrier state (Ahmed et al., 2010). The cell-specific promoters used included a previously characterized truncated form of the *Follicle stimulating hormone receptor* (*Fshr*) promoter (Griswold et al., 1995; Chodankar et al., 2005) and the *Müllerian inhibiting substance receptor type 2* (*Mis2r*) promoter (Josso et al., 2001; Connolly et al., 2003). The latter is expressed in the Müllerian ducts during embryological development, which later differentiate into internal reproductive organs including fallopian tubes, uterus, cervix, and a portion of the vagina, as well as other extra-uterine structures carrying increased cancer risk in *BRCA1* mutation carriers such as endosalpingiosis. *Mis2r* promoter is also active in mammary epithelium (Segev et al., 2001).

2. Materials and Methods

2.1. Ethics Statement

All studies with experimental animals were approved by and performed under supervision of the University of Southern California Institutional Animal Care and Use Committee.

2.2. Source and Handling of Experimental Animals

Animals were housed in a pathogen-free environment at the Vivaria facility of the USC Health Sciences campus. All facilities received daily monitoring and care from Vivaria staff under the supervision of a veterinarian. A maximum of 5 mice were housed per cage. Assignment to each experimental group was based on genotype. Euthanasia was achieved by cervical dislocation after the mice were made unconscious from exposure to CO₂.

2.3. Source or Generation and Characterization of Transgenic Mice and Constructs

The generation of *Fshr-Cre* transgenic mice was described earlier (Chodankar et al., 2005). This mouse is available from Jackson laboratory mouse repository (JAX Stock 24926, B6;D2-Tg(*Fshr-Cre*)1Ldu/J). Primers used for documenting the presence of the transgene were described (Chodankar et al., 2005). A 1.2 kb fragment of the *Mis2r* promoter provided by Dr. Connolly (Connolly et al., 2003) from the Fox Chase Cancer Center was placed upstream of either a 1.2 kb fragment of the β -galactosidase gene or a 1.1 kb *Cre* recombinase gene fragment,

followed by a 2.1 kb SV40 poly A tail. For the *Mis2r-Hsp68-lacZ* construct, a 0.9 kb fragment of the *Hsp68* minimal promoter was also placed downstream of the *Mis2r* promoter in a Bluescript KS vector backbone (Brugger et al., 2004). The linear purified construct was injected into the pronuclei of fertilized oocytes of B6D2F1 animals and the injected embryos were transferred into pseudopregnant mice according to standard protocols. Pups were analyzed for the presence of the *Cre* transgenic construct by PCR amplification of tail DNA using 5'-CTCTGGTGTAGCTGATGATC-3' as forward primer and 5'-TAATCGCCATCTCCAGCAG-3' as reverse primer. For detection of the *Mis2r-Hsp68-LacZ* construct we used a forward primer complementary to the *Mis2r* sequence (5'-ACAGAGACCGGGATAGGACAGA-3') and a reverse primer complementary to the *lacZ* sequence (5'-CAAACGGCGATTGACCGTA-3'). Founder mice were backcrossed with B6 animals to generate transgenic lines. Two independent transgenic lines were generated using each construct. *Mis2r-Cre* transgenic mice were crossed with either one of two R26R reporter lines, one carrying a *LacZ* gene whose expression requires excision of *loxP*-flanked stop sequences (*R26R^{LacZ}*) and the other carrying a similar floxed insert within the coding sequence for Green Fluorescence Protein (*R26R^{GFP}*). Signal to noise ratio and tissue specific expression were evaluated and compared in the various lines. The one with the highest level of tissue specific transgene expression was selected. Distribution of promoter activity was similar in transgenic lines generated independently from the same transgenic constructs.

2.4. Source and Genotyping of Mice Carrying Floxed Alleles

The mouse line carrying a floxed *p53* allele was purchased from the Jackson laboratory mouse repository (stock number 008,462). The unrearranged floxed allele was detected using 5'-GGTTAAACCCAGCTTGACCA-3' as forward PCR primer and 5'-GGAGGCAGAGACAGTTGGAG-3' as reverse primer. The *Cre*-driven rearrangement was detected using 5'-CACAAAAACAGGTTAAACCCA-3' as forward PCR primer and 5'-GAAGACAGAAAAAGGGAGGG-3' as reverse primer. The mouse line carrying a floxed *Brcal* allele targeting *Brcal* exon 11 was obtained from Chuxia Deng of the National Cancer Institute and genotyped as reported earlier (Chodankar et al., 2005).

2.5. Cre-mediated Recombination Analysis of R26R

Demonstration of β -galactosidase recombination was achieved first by enzymatic amplification of DNA from the organs of interest using 5'-AAAGTCGCTCTGAGTTGTTAT-3' and 5'-CAAACGGCGATTGACCGTA-3' as forward and reverse primers, respectively, followed by reamplification with 5'-AGTAAGGGAGCTGCAGTGGAGTA-3' and 5'-ATGGGATAGGTTACGTTGGTGTAGAT-3' as nested forward and reverse primers. Forward and reverse primers for detection of the unrearranged sequence were 5'-TTGCGCAGCTGTGCTCGACG-3' and 5'-AAGCGATGCCTGCGAATC-3'.

2.6. Colorimetric β -galactosidase Assay

Tissue samples were fixed in cold 4% paraformaldehyde, washed with cold phosphate buffered saline and dehydrated in 30% sucrose. Ten-micron cryostat sections were fixed in cold 0.2% glutaraldehyde. The sections were washed with cold phosphate buffered saline, preincubated in the same buffer containing 2 mM magnesium chloride, 0.01% sodium deoxycholate, 0.02% Nonidet P-40 for 10 min, and incubated overnight at 37 °C in 5 mM K₃Fe(CN)₆, 5 mM K₄Fe(CN)₆, 2 mM MgCl₂, 0.01% sodium deoxycholate, 0.02% Nonidet P-40, 1 mg/ml X-Gal (Sigma-Aldrich, St. Louis, MO, cat# B4252) in phosphate buffer saline [pH 7.4]. The sections were postfixed in 4% paraformaldehyde and counter stained with Nuclear Fast Red (Sigma-Aldrich, cat# 229113).

2.7. Determination of Age of Tumor Development

All mice were observed over a period of 24 months unless they developed a palpable tumor or showed signs of severe distress, such as due to underlying inflammatory conditions or to cancers outside the reproductive tract or the mammary glands such as lymphomas. All mice were fully necropsied. Age of detection of mammary tumors represents the age at which a palpable tumor was first detected. As for the 3 extra-uterine Müllerian cancers, age of detection refers to the age at which they were discovered incidentally at necropsy, including in a mouse that had reached the age of 24 months (accounting for one case), in a mouse that needed to be euthanized because of severe distress (one case), and in a mouse in which a mammary tumor had become palpable (one case).

2.8. Fluorescence Imaging

Green fluorescence in renal tissue sections was visualized with a Leica DMI 6000 inverted microscope and a 63× glycerol immersion objective (NA 1.4) and imaged using a Leica TCS SP5 AOBS confocal fluorescence imaging system powered by a Chameleon Ultra-II MP laser (Coherent Inc.) or a 488 nm Ar laser (Leica Microsystems). Fluorescence excitation and detector settings were the same for imaging transgenic and wild type tissue sections.

2.9. Laser Capture Microdissection

We used Arcturus XT-TI LCM System purchased from Arcturus BioScience Inc., Mountain View, California.

2.10. Immunohistochemical Detection of Estrogen and Progesterone Receptor Proteins

ER α (HC-20) and PR(AB-52) were purchased from Santa Cruz Biotechnology (catalogs #SC-543 and #SC-810, respectively, Santa Cruz, CA). Both antibodies were diluted 1:400 in 2.5% horse serum (in phosphate buffer saline) and hybridized to tissue sections overnight at 4 °C. Frozen tissue sections were fixed in 4% paraformaldehyde for 10 min followed by three 3-min washes in phosphate buffer saline, one 5 min incubation in 3% H₂O₂, and a 1-h incubation in 2.5% horse serum before incubation with the primary antibodies. The ImmPRESS Excel Staining kit, anti-rabbit Ig (catalog #MP-7601, Vector Laboratories, Burlingame, CA) was used for ER α according to manufacturer's instructions. Goat anti-mouse secondary antibody (catalogs # A11001, Invitrogen, Grand Island, NY, 1:400 in 2.5% horse serum, 1 h) was used as secondary antibody for PR immunostaining.

2.11. Her-2/neu Protein Detection by Western Blotting

Cells and tissues were lysed in triton lysis buffer (25 mM sodium phosphate, 150 mM sodium chloride, 1% Triton X-100, 5 mM EDTA, 50 mM sodium fluoride, 1 mM sodium vanadate, 1 mM phenylmethylsulfonyl fluoride, 5 μ M pepstatin A, 10 μ g/ml aprotinin, 10 μ g/ml leupeptin, 25 μ M phenylarsine oxide) for 30 min at 4 °C. Aliquots of 50 micrograms in Laemmli buffer were heated in boiling water for 5 min, electrophoresed on 10% polyacrylamide gels, and transferred to PVDF membranes (Biorad, Hercules, CA). The membranes were treated for one hour at room temperature with blocking buffer (5% milk proteins, 0.05% Tween 20 in Tris buffer, pH 8.1) and hybridized overnight in the same buffer containing 1:500 dilutions of rabbit anti-Neu (SC-284) and rabbit anti-GAPDH (SC-25,778) (both antibodies from Santa Cruz Biotechnology, Santa Cruz, CA). The membranes were washed 3 times for 5 min with 0.05% Tween-20 in Tris-Cl, pH 8.1 and probed with a 1:2000 dilution of goat anti-rabbit IgG-HRP (Santa Cruz Biotechnology, SC-2004) in blocking buffer for 1 h at room temperature. The membranes were then washed 3 times for 10 min in 0.05% Tween

20 in Tris buffer, pH 8.1 and incubated with ECL Western blot Substrate (ThermoFisher, Grand Island, NY, Catalog Number 32106) for 1 min before being exposed to X-ray films (Denville Scientific, Holliston, MA, Catalog Number E3012) for 5–10 min and developed.

3. Results

3.1. Distribution of *Mis2r* Promoter Expression in Tissues Derived From the Müllerian Ducts

3.1.1. Reproductive Organs

We first sought to verify that the *Mis2r* promoter in our proposed transgenic construct was active in tissues embryologically derived from the Müllerian ducts, the only anatomical structure currently known to express this receptor during development. Reproductive organs were obtained from 2-month old transgenic mice expressing β -galactosidase under the control of this promoter and stained for LacZ (Fig. 1a–d). The strong color seen over the cervix, uterine horns, and oviducts in the whole mount photograph shown in Fig. 1a, indicative of LacZ positivity, attests to the activity of the promoter in these organs at the time they were harvested. The ovaries, which are not embryologically derived from the Müllerian ducts, were also strongly positive. A cross section through a uterine horn in panel 1b shows LacZ positivity in the endometrial lining while the photograph in panel 1c shows positivity in the epithelial lining at the boundary between the cervix and upper vagina. Panel 1d shows absence of LacZ staining in a segment of uterine horn with attached oviduct and ovary from a non-transgenic littermate control.

3.1.2. Endosalpingiosis

We suggested earlier that structures derived from the most proximal portion of the Müllerian ducts, such as endosalpingiosis and others, are an important site of origin of tumors previously classified as ovarian carcinomas, including the high-grade serous subtype associated with the *BRCA1* mutation carrier state (Dubeau, 1999, 2008). We therefore sought to determine whether or not such structures express the *Mis2r* promoter in order to confirm their Müllerian origin and further evaluate the merit of this promoter as a driver of conditional *Bra1* inactivation in a mouse model for extra-uterine Müllerian tumor development. Staining intensity for LacZ in endosalpingiotic foci from mice carrying the *Mis2r-Hsp68-LacZ* transgene was weak and not convincingly above background levels. We therefore used a transgenic line expressing Cre recombinase under the control of *Mis2r*, which we crossed with the R26R line carrying the β -Galactosidase gene inactivated by a floxed insert containing a termination codon. Foci of endosalpingiosis, such as shown in Fig. 1e from a 3 day-old mouse, were obtained by laser capture microdissection and the presence or absence of Cre-mediated rearrangement was evaluated by PCR. A microdissected segment of uterine horn was used as positive control while microdissected ovarian surface epithelium was used as negative control. The results (Fig. 1f) confirmed that such rearrangement had taken place in the uterine horn and in endosalpingiosis while ovarian surface epithelium, previously regarded as the site of origin of most tumors classified as ovarian carcinoma, which we now classify as extra-uterine Müllerian carcinomas (Dubeau, 2008; Dubeau and Drapkin, 2013), showed no evidence of Cre-mediated rearrangement.

3.1.3. Renal Collecting System

A segment of the renal collecting ducts consistently stained positive for LacZ in R26R;*Mis2r-Cre* female, but not male mice as illustrated in Fig. 2a. These results are not due to endogenous LacZ activity in renal tissues because a similar conclusion was reached when we used a R26R mouse line where the β -Galactosidase sequence was replaced by that for *Green Fluorescence Protein* containing a floxed insert with a stop codon, allowing us to evaluate *Mis2r* promoter activity based on

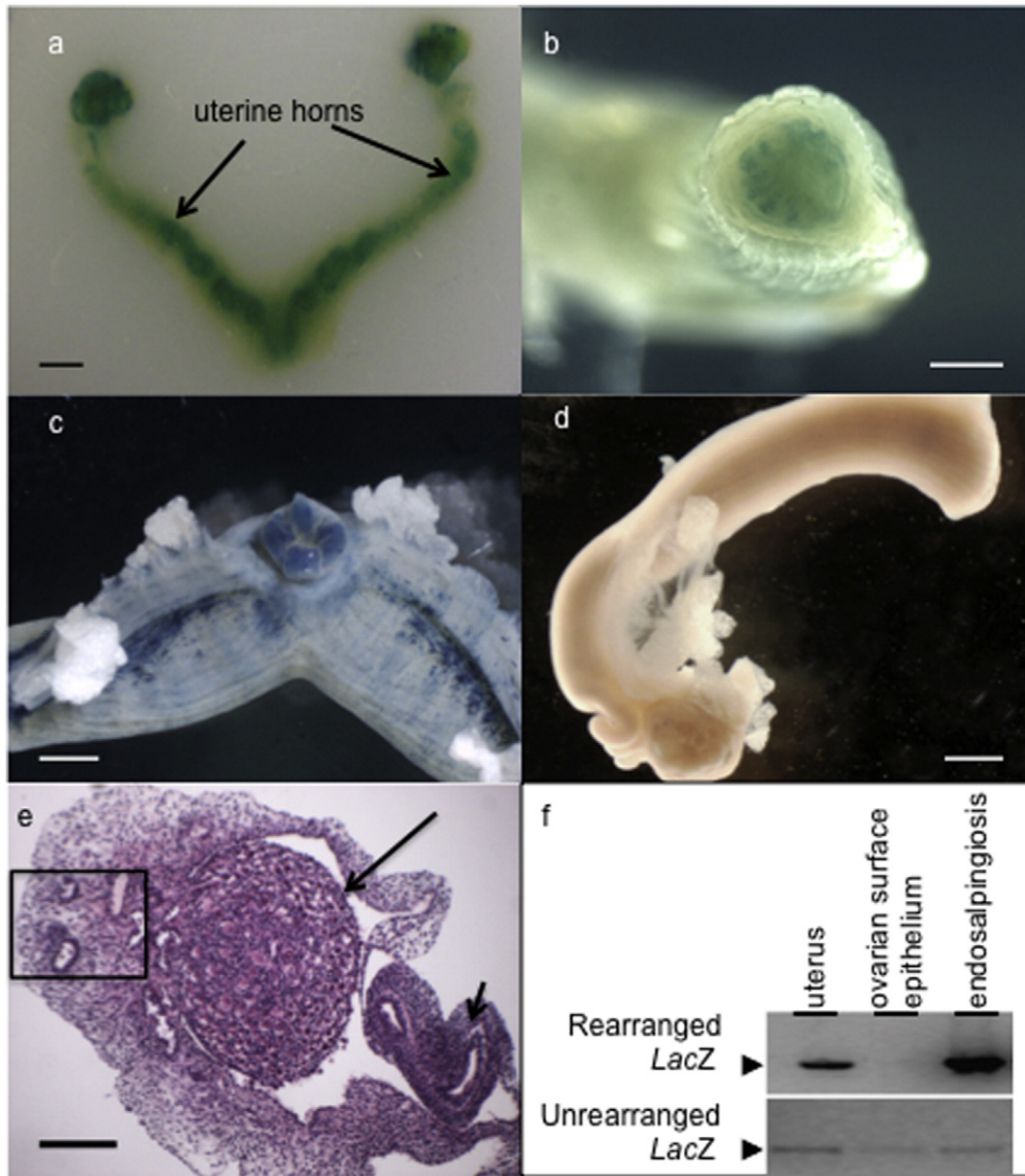


Fig. 1. *Mis2r* promoter expression in tissues embryologically derived from the Müllerian ducts. a–d: Reproductive organs from 2-month old *Mis2r-Hsp68-LacZ* transgenic mice and littermate controls were stained for LacZ, resulting in either green or blue reaction products. (a): Uterine horns (arrows) with attached ovaries from a transgenic animal. (b): Cross-section of uterine horns from the specimen shown in a. (c): Cross-section of upper part of vagina with attached segments of both uterine horns of a transgenic animal. (d): Segment of a uterine horn with attached ovary from a non-transgenic control. Scale bars: 1 mm. (e): Histological photograph of an ovary (long arrow) with adjacent uterine horn (short arrow) and foci of endosalpingiosis (rectangle) from a 2 day old *Mis2r-Cre;R26R^{LacZ}* mouse stained with hematoxylin and eosin. Scale bar: 200 μ m. Tissues of interest were subjected to laser capture microdissection. DNA was extracted and enzymatically amplified using PCR primers specific for either the rearranged or the unrearranged *LacZ* allele. The PCR products were electrophoresed on agarose gels and visualized under UV in order to examine the state of Cre-mediated rearrangement in each tissue (f).

fluorescence emission instead of LacZ staining (Fig. 2b). Given that Cre-mediated rearrangements are transmitted to daughter cells during mitosis, the presence of such rearrangements in either *R26R^{LacZ}* or *R26R^{GFP}* mice indicates that the *Mis2r* promoter has been active in renal collecting ducts or their embryological precursors at an undetermined time point before the mice were harvested, but does not necessarily reflect activity of this promoter at the time of euthanasia. Indeed, no renal tissue stained positive for LacZ in the *Mis2r-Hsp68-LacZ* line in either gender. The presence of gender-specific, Cre-mediated rearrangement in microdissected sections of histological preparation of renal tissue was also confirmed by PCR (Fig. 2c). These results strongly suggest a physical link between the Müllerian ducts and the renal collecting system early in development. This conclusion

is supported by an earlier report that the Wolffian ducts, the precursors of fetal (mesonephros) and adult (metanephros) renal systems, are in close relationship to each other in 12.5-day old mouse embryos (Kobayashi et al., 2003).

3.2. Distribution of *Mis2r* Promoter Expression in Tissues not Derived From the Müllerian Ducts

3.2.1. Ovaries

Strong LacZ positivity was seen over whole mounts of ovaries from *Mis2r-Hsp68-LacZ* mice in Fig. 1. We further investigated *Mis2r* promoter activity in this organ using *R26R* mice harboring the *Mis2r-Cre* transgene. As shown in Fig. 3, ovaries subjected to such staining procedures

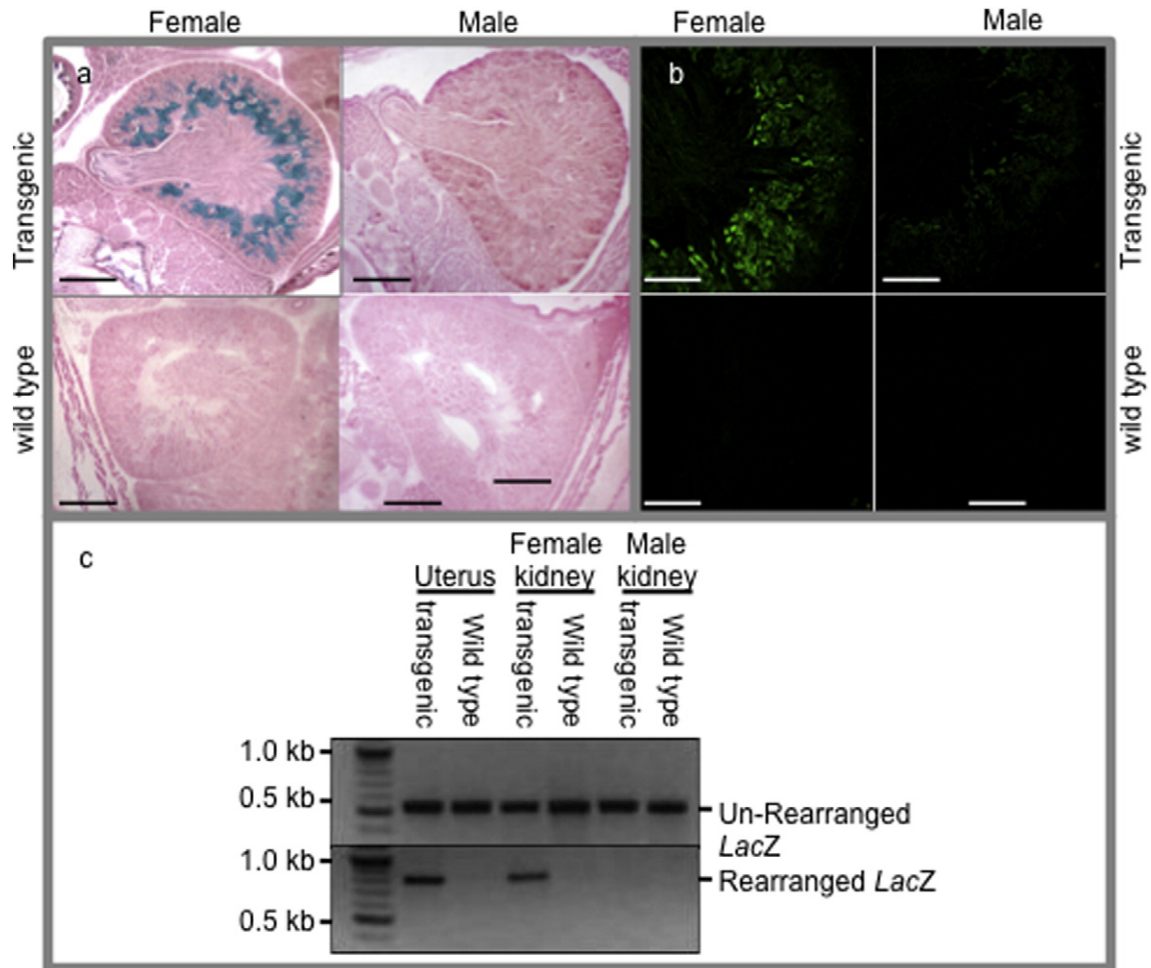


Fig. 2. Gender-specific expression of *Mis2r* in renal collecting ducts. Pelvic and lower abdominal tissues from male and female newborn $R26R^{LacZ}$ (a) or $R26R^{GFP}$ (b) reporter mice that either carried or did not carry the *Mis2r-Cre* transgene were exenterated and embedded as whole mounts, sectioned with a microtome, subjected to the LacZ staining protocol (a) or to fluorescent light (b), and examined by light microscopy. Tissue sections in (a) were counterstained with Nuclear Fast Red. Scale bars: 500 μ m. (c): DNA was extracted from the kidneys of newborn *Mis2r-Cre;R26R^{LacZ}* transgenic mice and from littermates lacking the *Mis2r-Cre* transgene. DNA extracted from the uterus of *Mis2r-Cre;R26R^{LacZ}* mice was used as positive control. The presence or absence of rearrangement of the β -galactosidase gene was documented by enzymatic amplification with the same primers used in Fig. 1f followed by electrophoresis on 1% agarose gels containing ethidium bromide and visualization of the PCR products under UV.

were strongly positive over their granulosa cell layers, in accordance with earlier reports of *Mis2r* expression in post-natal ovaries (Baarends et al., 1995). We suspected that LacZ positivity in ovarian follicles is not due to an embryological link between these follicles and the Müllerian ducts, but instead indicates acquisition of *Mis2r* expression during ovarian follicular differentiation. Although evidence of Cre-mediated rearrangement of the *R26R* allele could be detected by PCR as early as 3 days postnatally in *R26R;Mis2r-Cre* mice, no such rearrangement was detectable prenatally (Fig. 3c) in support of our hypothesis.

3.2.2. Mammary Gland

Strong LacZ positivity was also observed in the mammary glands of adult *Mis2r-Hsp68-LacZ* mice (Fig. 4), in support of earlier studies performed on adult human mammary glands (Segev et al., 2001). The presence of a physical interaction between mammary ducts and Müllerian ducts during development is highly unlikely given that the former are located outside the coelomic cavity. However, evidence of Cre-mediated rearrangement in the mammary glands of *R26R;Mis2r-Cre* mice was observed even in newborn animals (Fig. 4c–e), strongly suggesting that mammary ducts express *Mis2r* during their development, perhaps accounting for hormone-independent anatomical differences between male and female breasts.

3.3. Distribution of *Fshr* Promoter Expression in the Mammary Gland

Partial information on the distribution of activity of a truncated form of *Fshr*, which we previously used to investigate cell non-autonomous consequences of *Brca1* abnormalities, was reported earlier (Chodankar et al., 2005). We sought to expand these studies to investigate the expression status of this receptor in the mammary gland in order to further characterize our proposed mouse model. The results of Fig. 4g, which show a LacZ stain of an adult mammary gland obtained from *Fshr-Cre;R26R* mouse, clearly show expression in the mammary gland. Given earlier reports that this promoter, which is also active in ovarian granulosa cells, is not active in the fallopian tubes, we conclude that a *Brca1* gene knockout driven by *Fshr* can be a valuable tool to investigate cell non-autonomous consequences of *Brca1* inactivation in the Müllerian tract but not in the mammary gland.

3.4. Epithelial Tumor Development in Mice Carrying *Brca1* and *p53* Double Gene Knock Outs Driven by *Mis2r* and *Fshr* Promoters

Having characterized the distribution of *Mis2r* and *Fshr* promoter activity in relevant tissues, we tested the hypothesis that Müllerian and mammary tissues in mice carrying conditional *Brca1* and *p53* double mutations driven by these promoters are at increased risk of malignant

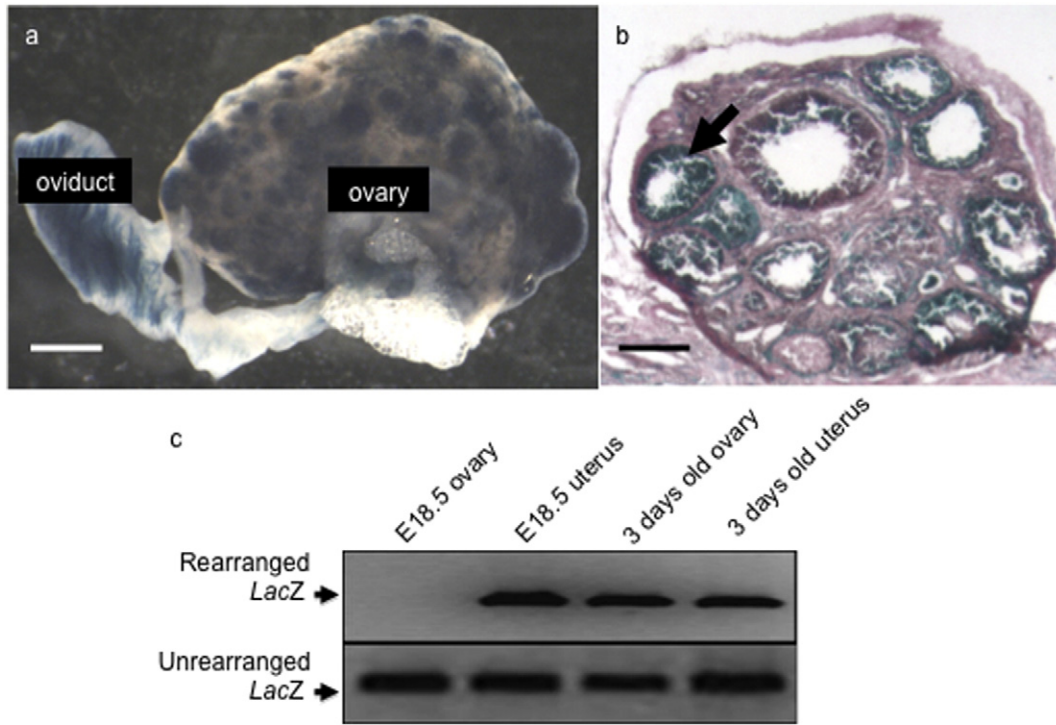


Fig. 3. Distribution of *Mis2r* promoter activity in mouse ovaries. Gross (a) and microscopic (b) photographs of ovaries from two 2-month-old *Mis2r-Cre* transgenic mice crossed with the *R26R^{LacZ}* reporter strain and stained for β -Gal. The arrow indicates LacZ positive pre-ovulatory ovarian follicles. (c): Genomic DNA samples from ovarian cortex and uterine tissues were extracted from *Mis2r-Cre;R26R^{LacZ}* reporter mice 2 days before birth (E18.5) and 3 days after birth and amplified enzymatically using PCR primers specific for either the rearranged or unrearranged β -galactosidase sequence. The PCR products were electrophoresed on 1% agarose gels containing ethidium bromide and visualized under UV. Scale bars: 200 μ m.

transformation. Mice carrying floxed alleles in *Brca1* and in *p53* were crossed with mice expressing either *Fshr-Cre* or *Mis2r-Cre* transgenes, or both of these transgenes. All double-mutant mice were fertile and had normal litter sizes. No evidence of malignancy was observed until the mice reached 10 months old. High-grade invasive tumors started

appearing at this time point in either mammary epithelium or in extra-uterine Müllerian epithelium. Representative examples of such tumors are shown in Fig. 5.

The frequency of mammary tumors based on the mutational state of *Brca1* and *p53* and on the nature of the transgenic construct utilized is

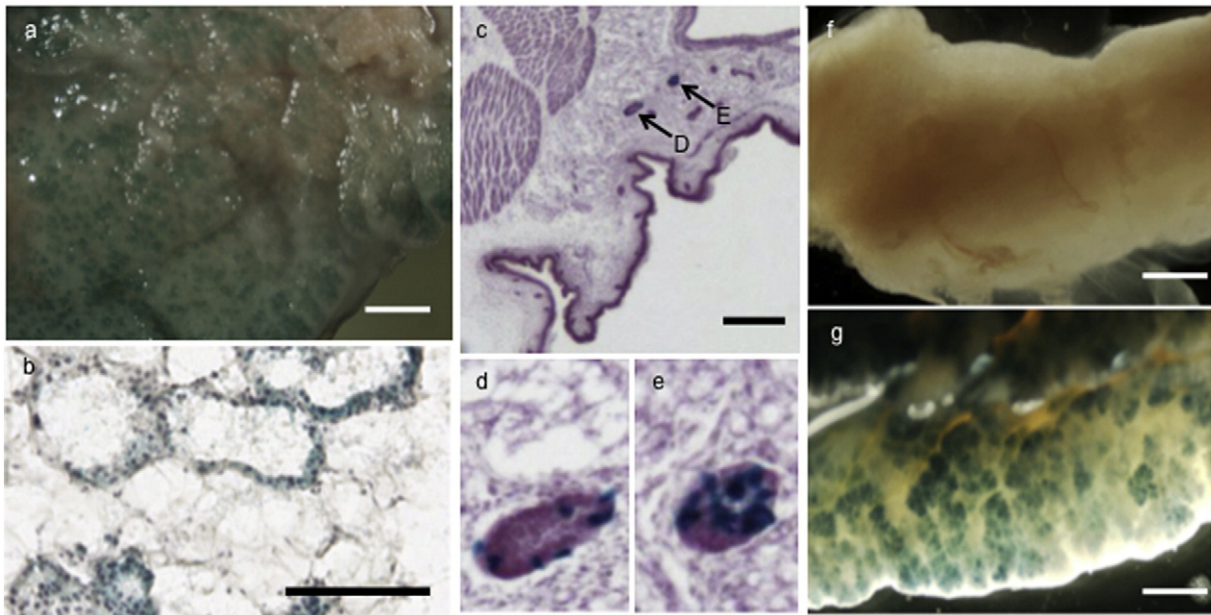


Fig. 4. *Mis2r* and *Fshr* promoter activity in the mammary gland. Mammary glands from an adult *Mis2r-Hsp68-lacZ* (a–b) mouse, a newborn (day 0) *Mis2r-Cre;R26R^{LacZ}* mouse (c–e), an adult *R26R^{LacZ}* mouse not carrying any transgene expressing Cre recombinase (f), and an adult *Fshr-Cre;R26R^{LacZ}* mouse (g) were stained for LacZ either as whole mounts (a, f–g) or after sectioning of frozen tissues with a cryostat (b–e). The tissue sections were counterstained with nuclear fast red. The arrows labeled D and E in panel c indicate glands that are magnified in panels d and e respectively. Magnification bars: 100 μ m in b, otherwise 200 μ m.

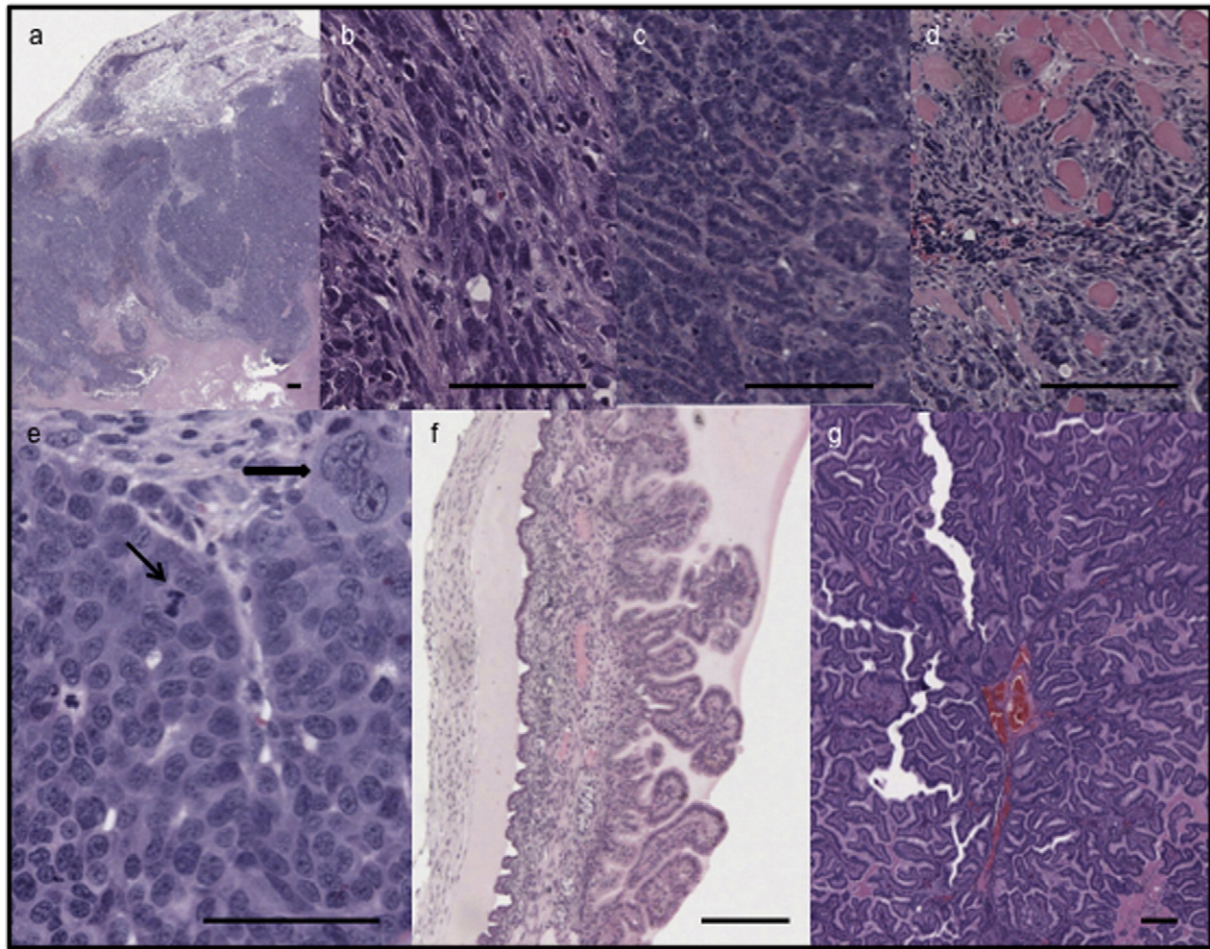


Fig. 5. Malignant transformation of mammary and extra-uterine Müllerian epithelium. An example of an invasive epithelial tumor of the mammary gland in a *Mis2r-Cre;Fshr-Cre;Brca1^{flox/flox};p53^{flox/flox}* mouse is shown in a. Different histological patterns of mammary tumors, including a solid tumor with spindloid features and a tumor showing tubular structures are shown in b and c respectively. (d): Infiltration of skeletal muscle by sheets of tumor cells. (e): High magnification of a solid tumor illustrating several classical features of malignant transformation including pleomorphic nuclei, atypical mitoses (thin arrow), and multinucleation (thick arrow). (f): Papillary tumor lining a pelvic extra-ovarian/extra-uterine cyst in a *Mis2r-Cre;Fshr-Cre;Brca1^{flox/flox};p53^{flox/flox}* mouse. Another papillary Müllerian tumor is shown in g. All tissues are stained with hematoxylin and eosin. Magnification bars: 50 µm in e, otherwise 100 µm.

shown in Table 1. Approximately 60% of mice carrying homozygous mutations in both of these genes developed such tumors. The majority of the tumors showed a solid pattern, with no evidence of acinar or tubular formation (Fig. 5a,b,e). Cancer-specific features readily apparent in

Fig. 5e include nuclear pleomorphism, atypical mitoses (thin arrow) and multinucleation (thick arrow). All tumors, regardless of genotype, showed high nuclear grade. In some tumors, the cells showed a spindloid appearance (Fig. 5b). Only 4 tumors showed tubular

Table 1
Effect of genotype on the frequency of mammary tumors.

Promoter	Number of mice with tumors/number of mice examined (age when tumor was first detected) ^a			
	<i>FshrMis2r</i>	<i>Fshr</i>	<i>Mis2r</i>	Total
<i>p53</i> ^{-/-} ; <i>Brca1</i> ^{-/-}	16/26 (13.8 ± 3.22 months)	2/5 (14.5 ± 1.5 months)	1/1 (10 months)	19/32 (13.7 ± 3.13 months)
<i>p53</i> ^{-/-} ; <i>Brca1</i> ^{+/+}	6/9 (15.4 ± 1.96 months)	0/3 (n/a)	2/4 (17.0 ± 1.00 months)	8/16 (15.9 ± 1.88 months)
<i>p53</i> ^{+/-} ; <i>Brca1</i> ^{-/-}	5/14 (16.3 ± 4.09 months)	4/8 (22.00 ± 3.46 months)	3/4 (20.7 ± 2.49 months)	12/26 (19.3 ± 4.38 months)
<i>p53</i> ^{-/-} ; <i>Brca1</i> ^{+/-}	3/9 (14.00 ± 1.63 months)	0/3 (n/a)	0/1 (n/a)	3/13 (14.00 ± 1.63 months)
<i>p53</i> ^{+/-} ; <i>Brca1</i> ^{+/-}	6/20 (17.7 ± 4.68 months)	0/7 (n/a)	1/2 (18 months)	7/29 (17.7 ± 4.33 months)
<i>p53</i> ^{+/-} ; <i>Brca1</i> ^{+/+}	0/9 (n/a)	0/9 (n/a)	0/7 (n/a)	0/25 (n/a)
Wild type	0/9 (n/a)	0/9 (n/a)	0/3 (n/a)	0/21 (n/a)

^a Age at which a palpable mammary tumor was first detected in living mice.

Table 2
Effect of genotype on the frequency of Müllerian tumors.

Promoter	Number of mice with tumors/number of mice examined (age when tumor-bearing mouse was euthanized) ^a			
	<i>Fshr Mis2r</i>	<i>Fshr</i>	<i>Mis2r</i>	Total
<i>p53</i> $-/-$; <i>Brca1</i> $-/-$	2/26 (18.0 ± 6.00 months)	0/5 (n/a)	0/1 (n/a)	2/32 (18.0 ± 6.00 months)
<i>p53</i> $-/-$; <i>Brca1</i> $+/+$	0/9 (n/a)	0/3 (n/a)	0/4 (n/a)	0/16 (n/a)
<i>p53</i> $+/+$; <i>Brca1</i> $-/-$	0/14 (n/a)	0/8 (n/a)	0/4 (n/a)	0/26 (n/a)
<i>p53</i> $-/-$; <i>Brca1</i> $+/-$	0/9 (n/a)	0/3 (n/a)	0/1 (n/a)	0/13 (n/a)
<i>p53</i> $+/+$; <i>Brca1</i> $+/-$	0/20 (n/a)	0/7 (n/a)	1/2 (18 months)	1/29 (18 months)
<i>p53</i> $+/-$; <i>Brca1</i> $+/+$	0/9 (n/a)	0/9 (n/a)	0/7 (n/a)	0/25 (n/a)
Wild type	0/9 (n/a)	0/9 (n/a)	0/3 (n/a)	0/21 (n/a)

^a Age at which tumors were discovered incidentally at necropsy, including in a mouse that had reached the age of 24 months (accounting for one case), in a mouse that needed to be euthanized because of general signs of distress (one case), and in a mouse in which a mammary tumor had become palpable (one case).

structures throughout the entire lesions (Fig. 5c) although a quarter of all mammary tumors contained some tubular structures within otherwise primarily solid lesions. No histological pattern was exclusive for any of the *Brca1* or *p53* mutational states. The invasive nature of the mammary lesions is illustrated in Fig. 5d, which shows infiltration of adjacent skeletal muscle by cancer cells.

The frequency of extra-uterine Müllerian tumors (Table 2) was substantially lower than that of mammary tumors, presumably due in part to the larger size of mammary glands compared to extra-uterine Müllerian structures, but also because mice with mammary tumors

were euthanized within 3 weeks of these tumors becoming grossly noticeable, preventing subsequent transformation of Müllerian epithelium. Mammary tumors were seen in mice harboring either the *Mis2r* or the *Fshr* transgenic promoters, alone or in combination (Table 1), but Müllerian tumors were not seen in mice harboring only the truncated *Fshr* transgenic promoter (Table 2), as expected given the lack of expression of this promoter in Müllerian epithelium as reported earlier (Chodankar et al., 2005). This underscores the potential utility of using mice in which Cre-mediated *Brca1* rearrangements are driven by this promoter to examine cell non-autonomous mechanisms of cancer

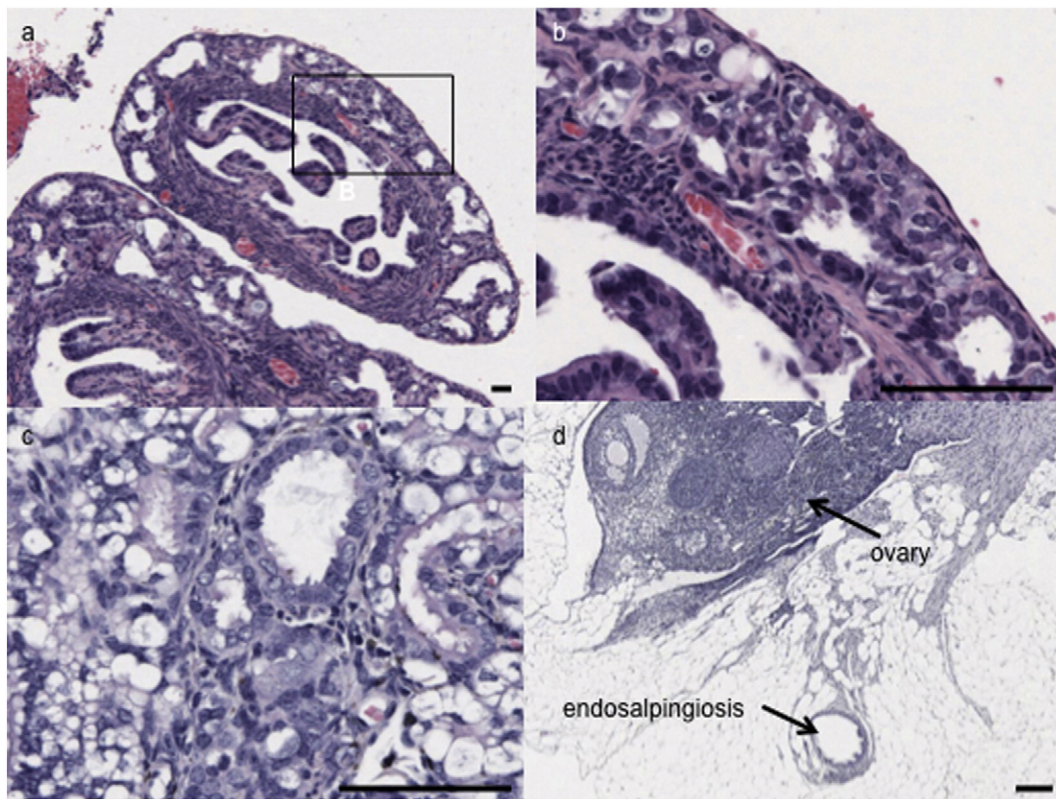


Fig. 6. Morphological evidence for an origin of extra-uterine tumors from endosalpingiosis. (a): sections of the distal oviducts, corresponding to the human fimbriae. The area within the rectangle is magnified in b. The sections show an invasive tumor surrounding the oviducts, but not involving the fimbrial epithelium. (c): focus of endosalpingiosis in peri-ovarian adipose tissue that shows crowded glands lined by atypical epithelial cells. d: prominent focus of endosalpingiosis in peri-ovarian adipose tissue, as typically seen in mice with mutant *Brca1*. Magnification bars: 50 μ m.

predisposition in the Müllerian tract. The origin of the Müllerian tumors was not confined to the fallopian tube, but included endosalpingiosis as evidenced from the photographs in Fig. 6, which show invasive tumors at the periphery of an otherwise intact fallopian tube (Fig. 6a–b) as well as a transformed focus of endosalpingiosis within peri-ovarian adipose tissue (Fig. 6c). In addition, mice in which no evidence of malignancy was detected in Müllerian organs commonly showed prominent endosalpingiosis (Fig. 6d). All extra-uterine Müllerian tumors were papillary and morphologically compatible with high grade serous carcinomas (Fig. 5f–g).

A substantial proportion (50%) of mice with a homozygous *p53* mutation carrying a functional *Brca1* allele also developed tumors, implying that some of the cancers observed in the double mutant mice may have been driven primarily by the mutant *p53* allele. The ages at which tumors developed in *p53* single knockout mice were not statistically different than in double knockouts ($P_{2\text{-tailed unpaired student t-test}} = 0.1142$, 95% confidence interval from -4.849 to 0.556). However, the influence of a mutant *Brca1* allele is underscored by the fact that although 46% of mice carrying a heterozygous *p53* mutation and a homozygous *Brca1* mutation developed malignancies, there was no tumor seen in mice heterozygous for a *p53* mutation and wild type for *Brca1* ($P < 0.0001$). Thus, the presence of a *Brca1* mutation was clearly instrumental in driving mammary tumors in double heterozygous mutants, which more closely mimic the genetic background of human *BRCA1* mutation carriers. Twenty eight percent of mice carrying heterozygous mutations in both, *p53* and *Brca1* developed either a mammary or an extra-uterine Müllerian tumor, providing a convenient level of penetrance to investigate environmental and cell non-autonomous risk factors for their human counterparts. The ages at which either *p53*^{+/-};*Brca1*^{+/+} or *p53*^{+/-};*Brca1*^{+/-} mice developed tumors were significantly higher than for *p53*^{-/-};*Brca1*^{-/-} mice ($P_{2\text{-tailed unpaired student t-test}} = 0.0004$ and 0.02 , respectively, confidence intervals from -8.437 to -2.725 and -7.321 to -0.687), presumably reflecting the need for additional genetic alterations, such as loss of the wild type *p53* and *Brca1* alleles via loss of heterozygosity (see below) for malignant transformation.

3.5. Pelvic Tumors Other Than in Extra-uterine Müllerian Epithelium

The promoters used to drive Cre recombinase in our mouse studies were not only expressed in mammary tissues and in extra-uterine Müllerian epithelium, but also in ovarian follicles, renal collecting system, and endometrium, at least at specific time points during embryological development or adult life (Figs. 1–3). Any of these tissues could potentially carry an elevated risk of cancer development in this mouse model. Indeed, 2 mice developed endometrial tumors that had

remained confined to the endometrium in our entire mouse cohort. None of the mice developed tumors of either ovarian follicles or renal ducts, underscoring the importance of cell-nonautonomous factors in determining risk of malignant transformation.

3.6. Second Mutational Event in Mice Carrying a Germline Heterozygous Mutation is Acquired via Loss of Heterozygosity

Most cancers that develop in human *BRCA1* mutation carriers harbor mutations in both alleles of this gene. The first mutation is acquired through the germline while the second is usually acquired via loss of heterozygosity, a common mechanism of tumor suppressor gene inactivation in general. We sought to determine whether a similar mechanism was associated with cancer development in mice carrying heterozygous *Brca1* or *p53* mutations in order to further evaluate the merit of this model as a tool to investigate human disease. DNA was extracted from mammary tumors of 3 different mice heterozygous for the floxed *Brca1* allele as well as from the tail of the same animals. Matched tail and tumor DNA samples were enzymatically amplified using primers for the *Ch11qB3* locus, a dinucleotide repeat microsatellite on mouse chromosome 11, which harbors both, the *p53* and *Brca1* loci. The primers were conjugated to a fluorescence-emitting chemical, allowing determination of the size of the PCR products following capillary electrophoresis. We suspected that the maternal and paternal alleles of microsatellite repeats might have different sizes given the mixed genetic background of the animals used to create this model. Indeed, 2 PCR products with major bands of respective sizes of 142 and 143 base pairs were seen in tail DNA from all 3 mice, as shown in the representative example in Fig. 7. Shadow bands of respective sizes of 140 and 141 base pairs are also present. The reduction in the intensity of the 142-base pair allele in DNA extracted from the tumor indicates loss of heterozygosity.

3.7. Sex Steroid Hormone Receptor and Her-2/neu Expression Status of Mammary Tumors

Breast cancers associated with the *Brca1* mutation carrier state in human are typically “triple negative” referring to their lack of expression of estrogen and progesterone receptors and absence of *Her-2/neu* amplification. We therefore examined the hormone receptor status of the mammary tumors seen in mice with either *p53* single knockouts or *p53/Brca1* double knockouts. Fig. 8 shows immunohistochemical stains for estrogen (top panels) and progesterone (bottom panels) receptors on 3 randomly selected mammary tumors for which frozen tissue samples were available, including 2 from mice carrying double *p53*

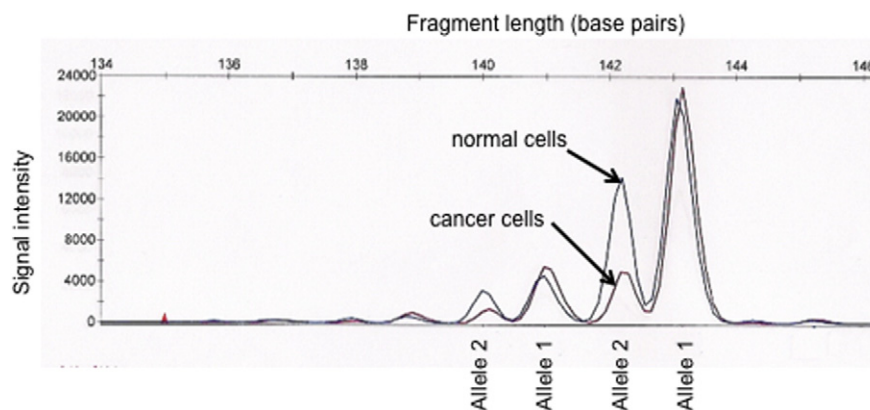


Fig. 7. Loss of heterozygosity on chromosome 11 in a mammary tumor from a mouse heterozygous for the floxed *Brca1* allele. DNA samples extracted from the tail (normal cells) or from a mammary tumor (cancer cells) of the same mouse were amplified by PCR using fluorescent primers for the *Ch11qB3* locus, a dinucleotide repeat polymorphism located on chromosome 11. Admixed normal cells accounted for approximately one third of the total cell population in the section of tumor. The PCR products were separated based on their sizes by capillary electrophoresis using an ABI 3500 Genetic Analyzer. The tracings show 2 alleles, of respective sizes of 142 and 143 base pairs in DNA extracted from normal cells, with 2 shadow bands 140 and 141 base pairs respectively. The 142 base pair allele, as well as the corresponding shadow band of 140 base pairs, is decreased in DNA extracted from the tumor, indicating loss of heterozygosity. These studies were repeated with 2 additional tumors and showed similar results (not shown).

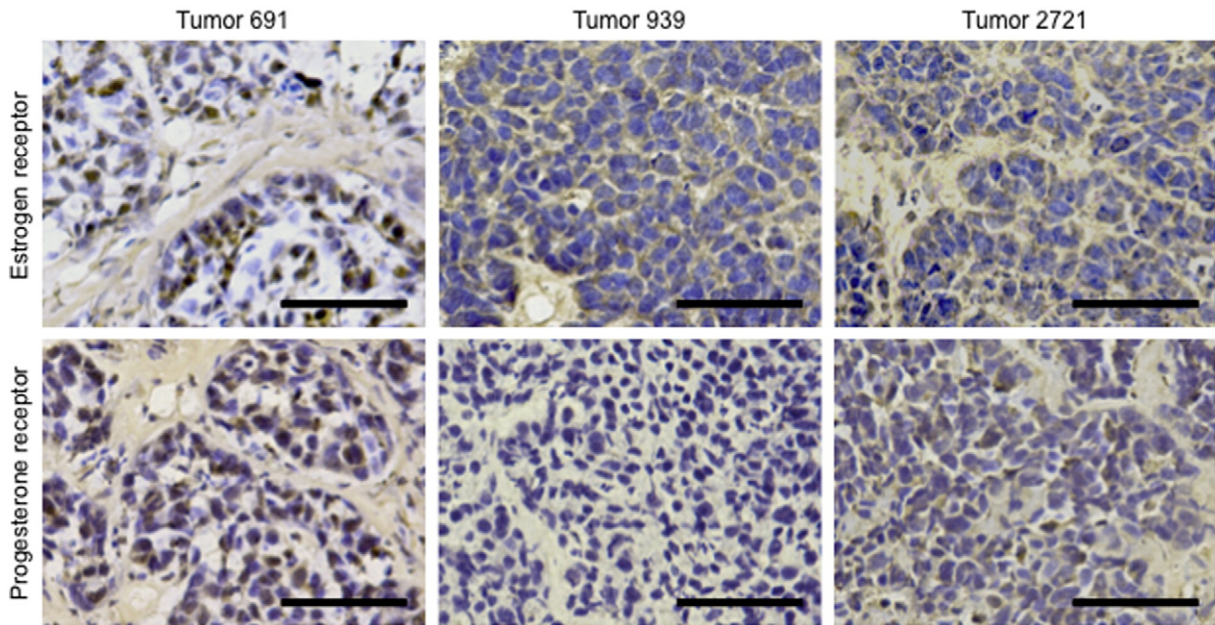


Fig. 8. Presence of estrogen and progesterone receptor proteins in mammary tumors from single versus double mutant mice. Three representative frozen sections of tumors derived from either a *p53* mutant (#691) or 2 *p53/Brca1* double mutants (#939 and #2721) were stained with antibodies directed against either estrogen (top panels) or progesterone (bottom panels) receptor proteins. Cre recombinase was driven by both the *Mis2r* and the *Fshr* transgenic promoters in all cases. Bars: 30 μ m.

and *Brca1* mutations (cases #939 and #2721) and one from a mouse carrying only a *p53* mutation (case #691). We were unable to obtain reliable stains on the remaining tumors, which had been fixed in formalin. The results show no evidence of estrogen receptor immunoreactivity in the tumors from double mutants while both, nuclear and cytoplasmic staining was present in the tumor from the mouse carrying a single knockout (Fig. 8). Progesterone receptor immunoreactivity was not seen in one of the 2 tumors derived from a double mutant mouse (#939) although it was detected in scattered tumor cells from the remaining such example shown in Fig. 8 (#2721). The tumor obtained

from a *p53* single mutant stained strongly for progesterone receptor (Fig. 8).

Protein extracts were also obtained from the same tumors and examined for Her-2/neu expression by Western blotting (Fig. 9). Expression of this protein was detected in all 3 tumors. The amount of expression was not higher than that seen in MCF-7 mammary carcinoma cells in which this oncogene is not amplified. We conclude that none of the 3 tumors show Her-2/neu amplification.

4. Discussion

We took advantage of 2 promoters with largely overlapping, but slightly different cell specificity to introduce conditional *Brca1* and *p53* double knockouts targeting the mammary gland, reproductive organs, and also organs playing a central role in controlling the estrous cycle, which is equivalent to the human menstrual cycle. The important drivers of estrous cycle activity targeted in this experimental model include ovarian granulosa cells and a subset of cells within the anterior pituitary. We had previously reported that *Brca1* inactivation in ovarian granulosa cells leads to changes in estrous cycle dynamics including prolongation of the pre-ovulatory phase and increased circulating levels of sex steroid hormones (Hong et al., 2010) and also reported on evidence that alterations in these hormonal levels are also present in human *BRCA1* mutation carriers (Widschwendter et al., 2013). Given the well-established importance of menstrual cycle activity as a risk modulator for breast and extra-uterine Müllerian carcinomas, our intention was to generate a mouse model suitable to investigate the interplay between genetic and hormonal factors of predisposition to both of these cancers. The truncated form of the *Fshr* promoter that we used in our studies is active in ovarian granulosa cells and in the anterior pituitary, both of which influence Müllerian tumorigenesis in a cell-nonautonomous manner, but it is not expressed in Müllerian epithelium (Chodankar et al., 2005). Thus, any contribution of genetic alterations driven by this promoter to Müllerian carcinogenesis can only be mediated through a cell-nonautonomous mechanism, hence its importance in our overall strategy.

Several transgenic or knockout models for extra-uterine Müllerian/ovarian and for mammary carcinomas have been developed over the

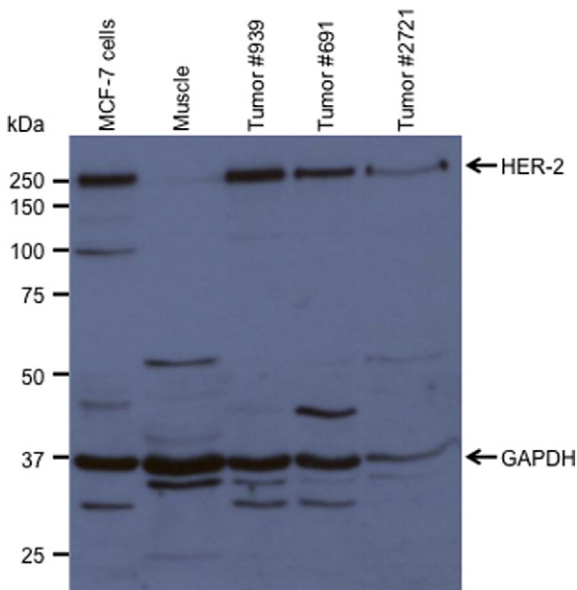


Fig. 9. Levels of Her-2/neu protein in mammary tumors. Protein extracts were obtained from MCF-7 cells derived from a human breast carcinoma lacking Her-2/neu amplification, from mouse muscle tissue (negative control), and from the 3 mammary carcinomas used in Fig. 8. The protein samples were analyzed by Western blotting using antibodies specific for Her-2/neu and Gapdh as well as for their respective human counterparts.

last 2 decades (see (Pfefferle et al., 2013; Hollern and Andrechek, 2014; Hasan et al., 2015) for reviews). In some cases, specific pathways, including Her-2/neu in mammary epithelium, Pten in Müllerian epithelium, and others have been targeted while others have focused on *Brca1/2* inactivation in tissues corresponding to those with an elevated cancer risk in human *BRCA1/2* mutation carriers. These contributions led to significant progress in our understanding of the cell-autonomous role of specific pathways in the development of these cancers. The model described here is associated with tumors that are morphologically similar to the human tumors associated with the *BRCA1/2* mutation carrier state, as evidenced by the high-grade papillary serous appearance of Müllerian tumors and the basal appearance and triple negative nature of at least some of the mammary tumors that we observed. This model is not based on targeting any specific signaling pathway, but on the inactivation of cell cycle regulators associated with human mammary and extra-uterine Müllerian cancer predisposition. It is also distinguished from existing models based on the following features: (1) it not only targets tissues similar to those at elevated risk of cancer in human *BRCA1/2* mutation carriers, but also organs that influence cancer predisposition from a distance via cell-nonautonomous mechanisms, closely mimicking the conditions associated with cancer predisposition in human *BRCA1* mutation carriers; (2) the fact that a significant proportion of mice heterozygous for *Brca1* and *p53* mutations develop tumors further increases similarities to the genetic background associated with human familial breast and extra-uterine Müllerian cancer predisposition; (3) the possibility of generating tumors in mice that are heterozygous for a *Brca1* mutation avoids confounders due to developmental defects associated with homozygous deletions of different splice forms of this gene, which have been reported both in the mammary gland and in the reproductive tract (Xu et al., 1999; Kim et al., 2006); (4) differences in the tissue specificity of the various promoters used to drive tissue-specific mutations, plus the possibility of using surgical manipulations entailing ovarian transplantation between mutant and wild type donors, make it possible to study cell-autonomous and the cell-nonautonomous mechanisms of cancer predisposition independently of each other and, therefore, to distinguish their respective contributions. Cell-nonautonomous mechanisms, which are mediated by circulating factors as opposed to intra-cellular changes, should be readily targetable pharmacologically, hence the importance of understanding their exact mechanisms.

Cell-autonomous and -nonautonomous effects in the mammary gland cannot be distinguished from each other simply by using different combinations of the *Mis2r* and *Fshr* promoters because both of these promoters are active in mammary epithelium. However, the fact that the *Fshr* promoter leads to cell-nonautonomous effects as previously documented (Chodankar et al., 2005; Hong et al., 2010; Yen et al., 2012) implies that mammary tumors are influenced by both mechanisms in the presence of both promoters, in contrast to existing models based on cell-autonomous strategies. Isolation of the cell-autonomous and cell-nonautonomous effects in order to investigate their relative roles is possible by performing ovarian transplantations from mutant donors into wild type recipients and *vice versa*, as we have done previously (Hong et al., 2010).

Mice carrying a mutation in *p53* but not in *Brca1* also developed mammary tumors, raising questions about the contribution of the *Brca1* mutation to cancer development in our double mutant animals. However, while mice carrying heterozygous mutations in both genes developed mammary tumors, none of the mice carrying only a heterozygous *p53* mutation developed such tumors, demonstrating that *Brca1* mutations are instrumental in driving tumor development in this model.

Three different groups have previously attempted to develop animal models for extra-uterine Müllerian carcinoma predisposition based on conditional knockouts of *Brca1* and *p53* driven in part by the *Mis2r* promoter (Clark-Knowles et al., 2009; Quinn et al., 2009; Xing et al., 2009). These investigators showed a high incidence rate of Müllerian sarcomas

in the double mutant mice, but did not report on the presence of any epithelial tumor. In contrast, a single sarcoma was seen in our mouse cohorts, in a mouse carrying a *p53* mutation and wild type *Brca1*. In 2 of those previous studies (Clark-Knowles et al., 2009; Quinn et al., 2009), the mutant mice carried deletions targeting a larger number of the exons of *Brca1* than in our mouse model that only targeted exon 11. However, this is unlikely to fully account for the phenotypic differences observed with these models because not only was the floxed *Brca1* allele used by Xing et al. (2009) identical to the one used in our studies, but also these authors used a transgenic construct driven by the *Mis2r* promoter to induce *Brca1* recombination. It is possible that differences in the nature of the *Mis2r-Cre* construct used by Xing et al., which was based on a knock-in strategy in contrast to our studies, may have led to differences in levels of promoter activity.

Our characterization of the tissue distribution of *Mis2r* promoter activity, led to the unexpected finding that a segment of the renal tubules, more specifically tubules located in the deep cortical area, show evidence of past *Mis2r* activity limited to females. These findings strongly suggest that a portion of the renal tubular system is embryologically linked to the Müllerian ducts, as supported by imaging studies of developing embryos reported by Kobayashi et al. (2003). The fact that different signaling molecules and transcription factors, such as *Lim*, *Pax2*, and *WT1*, are important regulators of both renal and Müllerian duct development provides further evidence for a link between these 2 organs (Mueller, 1994; Torres et al., 1995; Grote et al., 2006; Orvis and Behringer, 2007). This conclusion is also supported by the observation that congenital disorders associated with unilateral renal aplasia are often associated with absence of fallopian tube on the same side and unicornuate uterus on the other side (Grunwald, 1941). The presence of a developmental, embryological link between the Müllerian ducts and renal tubules may help explain gender differences in kidney function in health and disease, which is a topic of great current interest in renal (patho)physiology (Reckelhoff and Maric, 2010). These findings also have implications for the origin of the clear cell subtype of extra-uterine Müllerian carcinomas. All other major subtypes of these tumors can be readily associated with an extra-uterine Müllerian epithelial structure of a similar differentiation lineage (Dubeau, 2008). Tumors belonging to the clear cell subtype not only show morphological resemblances to clear cell carcinomas of the kidneys, but also their gene expression profile has been reported to share similarities with that of these tumors (Zorn et al., 2005). These cancers also share similarities in their response to chemotherapy (Anglesio et al., 2011). The adult (metanephros) and fetal (mesonephros) kidneys are both derived from the pronephric duct (Pole et al., 2002; Pietila and Vainio, 2005). In addition, the mesonephric ureteric bud is a driver of metanephros development (Sainio et al., 1997), underscoring an embryological link between the mesonephros and metanephros. Different signaling molecules and transcription factors, such as *Lim*, *Pax2*, and *WT1*, are important regulators of both renal and Müllerian duct development (Mueller, 1994; Torres et al., 1995; Grote et al., 2006; Orvis and Behringer, 2007), providing further evidence for a link between these 2 organs. We therefore propose that mesonephric remnants, which are abundant in the para-ovarian and para-tubal areas, should be regarded as integral components of extra-uterine Müllerian epithelium and may play a role in the histogenesis of clear cell carcinomas.

Our findings have implications on the site of origin of serous extra-uterine Müllerian carcinomas, which until recently were thought to originate primarily from metaplastic foci within the ovarian surface mesothelium (Dubeau, 1999, 2008). The fallopian tube is currently regarded as the most important site of origin of these tumors, the type associated with the *BRCA1* mutation carrier state. We argued earlier that other extra-uterine Müllerian structures, including endosalpingiosis, endometriosis, and endocervicosis are also important in the histogenesis of the serous, endometrioid, and mucinous subtypes, respectively (Dubeau, 1999, 2008; Ahmed et al., 2010; Dubeau and Drapkin, 2013). All pelvic tumors seen in our mouse cohort appeared

to have originated from endosalpingiosis, indicating that such extra-uterine structures are at risk of cancer development in mice carrying mutations mimicking those present in human with familial extra-uterine Müllerian carcinoma in support of our hypothesis.

In summary, we developed a mouse model that recapitulates the cell-autonomous and cell-nonautonomous mechanisms of cancer predisposition in human *BRCA1* carriers. This model should facilitate elucidation of the menstrual factors associated with cell-nonautonomous mechanisms, which could represent attractive targets for cancer prevention strategies. Characterization of this model led to insights into the role of endosalpingiosis in the histogenesis of high grade serous extra-uterine Müllerian tumors, previously called ovarian, which should be considered in developing early detection and risk-reducing surgical strategies for these tumors. Our findings also shed light on the differentiation lineage of Müllerian clear cell carcinomas, which may facilitate the development of novel therapeutic approaches.

Funding Source Statement

No funding source played any role in the writing of the manuscript or in data collection or analysis.

Author's Contributions

Ying Liu developed the mouse model, made the *Mis2r-Cre* and *Mis2r-Hsp68-LacZ* constructs, maintained the mouse colonies, performed all autopsies, performed most of the experiments, and participated in the overall planning. Hai-Yun Yen performed the immunostains for estrogen and progesterone receptor proteins. Theresa Austria performed the studies on Her-2/neu expression. Jonas Pettersson performed studies on loss of heterozygosity. Janos Peti-Peterdi helped with the imaging studies of the kidney and helped in the redaction of the manuscript. Robert Maxson helped in the designing of the transgenic constructs and participated in the redaction of the manuscript. Martin Widschwendter helped in the analysis of the data and in the redaction of the manuscript. Louis Dubeau conceived and supervised the entire project and wrote the initial draft of the manuscript.

Acknowledgments

This work was aided by grants R01 CA119078 and R01 CA133117 from the US National Institutes of Health and by a gift from the Ovarian Cancer Coalition of Greater California to LD. Part of this work was funded by the Eve Appeal and undertaken at UCLH/UCL, which received a proportion of its funding from the Department of Health NIHR Biomedical Research Centers (BRC) funding scheme.

References

Ahmed, A.A., et al., 2010. Driver mutations in TP53 are ubiquitous in high grade serous carcinoma of the ovary. *J. Pathol.* 221, 49–56.

Anglesio, M.S., et al., 2011. IL6-STAT3-HIF signaling and therapeutic response to the angiogenesis inhibitor sunitinib in ovarian clear cell cancer. *Clin. Cancer Res.* 17, 2538–2548.

Baarends, W.M., Uilenbroek, J.T., Kramer, P., Hoogerbrugge, J.W., van Leeuwen, E.C., Themmen, A.P., Grootegeod, J.A., 1995. Anti-Müllerian hormone and anti-Müllerian hormone type II receptor messenger ribonucleic acid expression in rat ovaries during postnatal development, the estrous cycle, and gonadotropin-induced follicle growth. *Endocrinology* 136, 4951–4962.

Boyle, P., Levin, B. World Cancer Report 2008. International Agency for Research on Cancer aWHO, Editor. Geneva, Switzerland: WHO Press; 2008.

Brose, M.S., Rebbeck, T.R., Calzone, K.A., Stopfer, J.E., Nathanson, K.L., Weber, B.L., 2002. Cancer risk estimates for BRCA1 mutation carriers identified in a risk evaluation program. *J. Natl. Cancer Inst.* 94, 1365–1372.

Brugger, S.M., et al., 2004. A phylogenetically conserved cis-regulatory module in the *Msx2* promoter is sufficient for BMP-dependent transcription in murine and drosophila embryos. *Development* 131, 5153–5165.

Chodankar, R., et al., 2005. Cell-nonautonomous induction of ovarian and uterine serous cystadenomas in mice lacking a functional *brca1* in ovarian granulosa cells. *Curr. Biol.* 15, 561–565.

Clark-Knowles, K.V., Garson, K., Jonkers, J., Vanderhyden, B.C., 2007. Conditional inactivation of *Brca1* in the mouse ovarian surface epithelium results in an increase in preneoplastic changes. *Exp. Cell Res.* 313, 133–145.

Clark-Knowles, K.V., Senterman, M.K., Collins, O., Vanderhyden, B.C., 2009. Conditional inactivation of *Brca1*, *p53* and *Rb* in mouse ovaries results in the development of leiomyosarcomas. *PLoS One* 4, e8534.

Connolly, D.C., Bao, R., Nikitin, A.Y., Stephens, K.C., Poole, T.W., Hua, X., Harris, S.S., Vanderhyden, B.C., Hamilton, T.C., 2003. Female mice chimeric for expression of the simian virus 40 Tag under control of the MISIR promoter develop epithelial ovarian cancer. *Cancer Res.* 63, 1389–1397.

Dinulescu, D.M., Ince, T.A., Quade, B.J., Shafer, S.A., Crowley, D., Jacks, T., 2005. Role of *K-ras* and *Pten* in the development of mouse models of endometriosis and endometrioid ovarian cancer. *Nat. Med.* 11, 63–70.

Dubeau, L., 1999. The cell of origin of ovarian epithelial tumors and the ovarian surface epithelium dogma: does the emperor have no clothes? *Gynecol. Oncol.* 72, 437–442.

Dubeau, L., 2008. The cell of origin of ovarian epithelial tumours. *Lancet Oncol.* 9, 1191–1197.

Dubeau, L., Drapkin, R., 2013. Coming into focus: the nonovarian origins of ovarian cancer. *Ann. Oncol.* 24 (Suppl. 8), viii28–viii35.

Flesken-Nikitin, A., Choi, K.-C., Eng, J.P., Schmidt, E.N., Nikitin, A.Y., 2003. Induction of carcinogenesis by concurrent inactivation of *p53* and *Rb1* in the mouse ovarian surface epithelium. *Cancer Res.* 63, 3459–3463.

Griswold, M.D., Heckert, L., Linder, C., 1995. The molecular biology of the FSH receptor. *J. Steroid Biochem. Mol. Biol.* 53, 215–218.

Grote, D., Souabni, A., Busslinger, M., Bouchard, M., 2006. Pax 2/8-regulated *Gata 3* expression is necessary for morphogenesis and guidance of the nephric duct in the developing kidney. *Development* 133, 53–61.

Grunwald, P., 1941. The relation of the growing Mullerian duct to the Wolffian duct and its importance for the genesis of malformations. *Anat. Rec.* 81, 1–19.

Hasan, T., Carter, B., Denic, N., Gai, L., Power, J., Voisey, K., Kao, K.R., 2015. Evaluation of cell-line-derived xenograft tumours as controls for immunohistochemical testing for ER and PR. *J. Clin. Pathol.* 68, 746–751.

Hollern, D.P., Andrechek, R., 2014. A genomic analysis of mouse models of breast cancer reveals molecular features of mouse models and relationships to human breast cancer. *Breast Cancer Res.* 16, R59.

Hong, H., Yen, H.Y., Brockmeyer, A., Liu, Y., Chodankar, R., Pike, M.C., Stanczyk, F.Z., Maxson, R., Dubeau, L., 2010. Changes in the mouse estrus cycle in response to *Brca* inactivation suggest a potential link between risk factors for familial and sporadic ovarian cancer. *Cancer Res.* 70, 221–228.

Josso, N., di Clemente, N., Gouedart, L., 2001. Anti-Müllerian hormone and its receptors. *Mol. Cell. Endocrinol.* 179, 25–32.

Kim, S.S., Cao, L., Lim, S.C., Li, C., Wang, R.H., Xu, X., Bachelier, R., Deng, C.X., 2006. Hyperplasia and spontaneous tumor development in the gynecologic system in mice lacking the *BRCA1-Delta11* isoform. *Mol. Cell. Biol.* 26, 6983–6992.

Kobayashi, A., Shawlot, W., Kania, A., Behringer, R.R., 2003. Requirement of *Lim1* for female reproductive tract development. *Development* 131, 539–549.

Miyoshi, I., Takahashi, K., Kon, Y., Okamura, T., Mototani, Y., Araki, Y., Kasai, N., 2002. Mouse transgenic for murine oviduct-specific glycoprotein promoter-driven simian virus 40 large T-antigen: tumor formation and its hormonal regulation. *Mol. Reprod. Dev.* 63, 168–176.

Mueller, R.F., 1994. The Denys-Drash syndrome. *J. Med. Genet.* 31, 471–477.

Narod, S.A., et al., 1998. Oral contraceptives and the risk of hereditary ovarian cancer. *N. Engl. J. Med.* 424–428.

Orsulic, S., Li, Y., Soslow, R.A., Vitale-Cross, L.A., Gutkind, J.S., Varmus, H.E., 2002. Induction of ovarian cancer by defined multiple genetic changes in a mouse model system. *Cancer Cell* 1, 53–62.

Orvis, G.D., Behringer, R.R., 2007. Cellular mechanisms of Mullerian duct formation in the mouse. *Dev. Biol.* 306, 493–504.

Perets, R., et al., 2013. Transformation of the fallopian tube secretory epithelium leads to high-grade serous ovarian cancer in *Brca1*; *Tp53*; *Pten* models. *Cancer Cell* 24, 751–765.

Pfefferle, A.D., et al., 2013. Transcriptomic classification of genetically engineered mouse models of breast cancer identifies human subtype counterparts. *Genome Biol.* 14, R125.

Pietila, I., Vainio, S., 2005. The embryonic aorta-gonad-mesonephros region as a generator of haematopoietic stem cells. *APMIS* 113, 804–812.

Pike, M.C., Pearce, C.L., Peters, R., Cozen, W., Wan, P., Wu, A.H., 2004. Hormonal factors and the risk of invasive ovarian cancer: a population-based case-control study. *Fertil. Steril.* 82, 186–195.

Pole, R.J., Qi, B.Q., Beasley, S.W., 2002. Patterns of apoptosis during degeneration of the pronephros and mesonephros. *J. Urol.* 167, 269–271.

Quinn, B.A., Brake, T., Hua, X., Baxter-Jones, K., Litwin, S., Hedrick Ellenson, L., Connolly, D.C., 2009. Induction of ovarian leiomyosarcomas in mice by conditional inactivation of *Brca1* and *p53*. *PLoS One* 4, e8404.

Reckelhoff, J.F., Maric, C., 2010. Sex and gender differences in cardiovascular-renal physiology and pathophysiology. *Steroids* 75, 745–746.

Sainio, K., Hellstedt, P., Kreidberg, J.A., Saxen, L., Sariola, H., 1997. Differential regulation of two sets of mesonephric tubules by *WT-1*. *Development* 124, 1293–1299.

Segev, D.L., Hoshiya, Y., Stephen, A.E., Hoshiya, M., Tran, T.T., MacLaughlin, D.T., Donahoe, P.K., Maheswaran, S., 2001. Mullerian inhibiting substance regulates *NFκB* signaling and growth of mammary epithelial cells in vivo. *J. Biol. Chem.* 276, 26799–26806.

Szabova, et al., 2012. Perturbation of *Rb*, *p53*, and *Brca1* or *Brca2* cooperate in inducing metastatic serous epithelial ovarian cancer. *Cancer Res.* 72, 4141–4153.

Torres, M., Gomez-Pardo, E., Dressler, G.R., Gruss, P., 1995. Pax-2 controls multiple steps of urogenital development. *Development* 121, 4057–4065.

Whittemore, A.S., Harris, R., Itytre, J., 1992. Characteristics relating to ovarian cancer risk: collaborative analysis of 12 US case-control studies. II. Invasive epithelial ovarian

- cancers in white women. Collaborative Cancer Group. *Am. J. Epidemiol.* 136, 1184–1203.
- Widschwendter, M., et al., 2013. The sex hormone system in carriers of Brca1/2 mutations: a case–control study. *Lancet Oncol.* 14, 1226–1232.
- Xing, D., et al., 2009. A role for BRCA1 in uterine leiomyosarcoma. *Cancer Res.* 69, 8231–8235.
- Xu, X., Wagner, K.-U., Larson, D., Weaver, Z., Li, C., Ried, T., Hennighausen, L., Wynshaw-Boris, A., Deng, C.-X., 1999. Conditional mutation of Brca1 in mammary epithelial cells results in blunted ductal morphogenesis and tumour formation. *Nat. Genet.* 22, 37–43.
- Yen, H.Y., Gabet, Y., Liu, Y., Martin, A., Wu, N.L., Pike, M.C., Frenkel, B., Maxson, R., Dubeau, L., 2012. Alterations in Brca1 expression in mouse ovarian granulosa cells have short-term and long-term consequences on estrogen responsive organs. *Lab. Investig.* 92, 802–811.
- Zorn, K.K., Bonome, T., Gangi, L., Chandramouli, G.V., Awtrey, C.S., Gardner, G.J., Barrett, J.C., Boyd, J., Birrer, M.J., 2005. Gene expression profiles of serous, endometrioid, and clear cell subtypes of ovarian and endometrial cancer. *Clin. Cancer Res.* 11, 6422–6430.